# 모델의 불확실성이 구조물의 손상예측정확도에 미치는 영향

# Damage Prediction Accuracy as a Function of Model Uncertainty in Structures

김 정 태*
Kim, Jeong-Tae

요 약

구조물의 손상예측정확도를 모델불확실성의 함수로 산정하는 방법론이 제시되었다. 먼저, 구조물의 손상발생위치와 크기를 결정할 수 있는 알고리즘이 요약되고 모델불확실성과 손상발견정확도를 측정하는 방법들이 제시되었다. 다음으로, 실존구조물의 손상발견정확도에 미치는 모델불확실성의 영향을 산정하는 방법론이 제시되었다. 마지막으로, 한개의 진동모드가 측정된 Plate-Girder 교량을 사용하여 이같은 산정방법론의 적합성이 예증되었다.

Abstract

A methodology to assess damage prediction accuracy as a function of model uncertainty in structures is presented. In the first part, a theory of approach is outlined. First, a damage detection algorithm to locate and size damage in structures using few modal responses of the structures is summarized. Next, methods to quantify model uncertainty and the damage detection accuracy are formulated. In the second part, a methodology to assess the effect of model uncertainty on the damage detection accuracy of real structures is designed. In the last part, the feasibility of the assessment methodology is demonstrated by using a plate-girder bridge for which only information on a single mode is available.

* Postdoctoral Research Associate, Department of Civil Engineering, Texas A&M University, College Station, TX 77843, USA

이 논문에 대한 토론을 1995년 3월 31일까지 본 학회에 보내주시면 1995년 9월호에 그 결과를 게재하겠습니다.

## 1. INTRODUCTION

During the past decade, many research studies have focused on the possibility of using the vibration characteristics of structures as an indication of structural damage[1,2,3]. More recently, attempts have been made to monitor structural integrity of bridges[4], and to investigate the feasibility of damage detection in large space structures using changes in modal parameters[5]. Studies have also attempted to investigate model uncertainty in structural systems[6] and to evaluate the effect of model uncertainty on damage detection accuracy in beams[7]. Despite these combined research efforts, there are still outstanding needs : e.g., to detect damage in structures with limited modal information and to evaluate the damage in an environment of uncertainty due to modeling errors and modal response measurement errors. Solutions to these problems are important because a timely damage assessment could save lives and property, increase structural reliability and productivity of operations, and reduce maintenance costs.

The objective of this paper is to present a methodology to evaluate the relative impact of model uncertainty on the accuracy of nondestructive damage detection (NDD) in structures. Here, model uncertainty is defined as a lack of knowledge regarding the topology, geometry, material properties, and dynamic modal responses of the structure. The accuracy is defined as the degree of conformity of a measure to a true value (i.e., a measure of errors). Relative impact of a model uncertainty is meant by the size of the effect of model uncertainty relative to the different causes. In order to achieve the objective, the investigation is performed in three parts. In the first part, a theory of approach is outlined. First, a theory of damage localization and severity estimation which yields information on locations and magnitudes of damage directly from changes in mode shapes of structures is formulated. Next, a system identification method to generate a theoretical model (i.e., a realistic, but simplified, mathematical representation) of a structure is formulated. Finally, methods to quantify model uncertainty and the damage detection accuracy are formulated. In the second part, a methodology to estimate the relative effect of model uncertainty on the damage detection accuracy of structures is designed. In the last part, the feasibility of the assessment methodology is demonstrated by using a plate-girder bridge for which only information on a single mode is available. The accuracy of damage prediction results of the plate-girder bridge is assessed as a function of model uncertainties which may exist in the damage detection procedures of the bridge.

## 2. THEORY OF APPROACH

### 2.1 Theory of Damage Localization and Severity Estimation

Consider a linear, undamaged, skeletal structure with NE elements and N nodes. The $i^{th}$ modal stiffness, $K_i$, of the arbitrary structure is given by[8]

$$K_i = \Phi_i^T \mathbf{C} \Phi_i \tag{1}$$

where $\Phi_i$ is the $i^{th}$ modal vector and $\mathbf{C}$ is the system stiffness matrix. The contribution of the $j^{th}$ member to the $i^{th}$ modal stiffness, $K_{ij}$, is given by

$$K_{ij} = \Phi_i^T \mathbf{C}_j \Phi_i \tag{2}$$

where $\mathbf{C}_j$ is the contribution of $j^{th}$ member to the system stiffness matrix. Then, the sensitivity (i.e., the fraction of modal energy) of $i^{th}$ mode and $j^{th}$ member is given by

$$F_{ij}=K_{ij}/K_i \tag{3}$$

Let the corresponding modal parameters in Eqs. 1 to 3 associated with a subsequently damaged structure be characterized by asterisks. Then for the damaged structure

$$F^*_{ij}=K^*_{ij}/K^*_i \; ; \; [K^*_{ij}=\Phi^{*T}_i \mathbf{C}^*_j \Phi^*_i, \; K^*_i=\Phi^{*T}_i \mathbf{C}^* \Phi^*_i] \tag{4}$$

Dividing Eq. 4 by Eq. 3 yields

$$\frac{F^*_{ij}}{F_{ij}}=\frac{K^*_{ij}}{K_{ij}}\frac{K_i}{K^*_i} \tag{5}$$

The quantities $\mathbf{C}_j$ and $\mathbf{C}^*_j$ in Eq. 2 and Eq. 4 may be written as follows ;

$$\mathbf{C}_j=E_j\mathbf{C}_{jo} \; ; \; \mathbf{C}^*_j=E^*_j\mathbf{C}_{jo} \tag{6}$$

where $E_j$ is a parameter representing the material stiffness properties and the matrix $\mathbf{C}_{jo}$ involves only geometric quantities (and possibly terms containing Poisson's ratio). Suppose an approximation that the fraction of modal energy is the same for both damaged and undamaged structures, on substituting Eq. 6 into Eq. 5 and rearranging, then a damage index $\beta_j$ of $j^{th}$ member is obtained by (see Reference [8] for details)

$$\beta_j=\frac{E_j}{E^*_j}=\frac{[\Phi^{*T}_i C_{jo}\Phi^*_i]}{[\Phi^T_i C_{jo}\Phi_i]}\frac{K_i}{K^*_i} \tag{7}$$

where damage is indicated at the $j^{th}$ member if $\beta_j>1$. All quantities on R.H.S. of Eq. 7 can be obtained from the experimental measurements and the geometry of the structure.

Now, damage locations are decided on the basis of a rejection of hypotheses in the statistical sense. The $\beta_j$ is treated as a realization of a random variable $\beta$ for $i^{th}$ mode. Then the damage localization indicator is given by

$$Z_j=(\beta_j-\bar{\beta}_i)/\sigma_i \tag{8}$$

in which $\bar{\beta}_i$ and $\sigma_i$ represent, respectively, the mean and the standard deviation of $\beta$ for $i^{th}$ mode. The existence of damage is investigated by testing two hypotheses : (1) no damage is present in $j^{th}$ member (i.e., $H_o$) and (2) damage is present in $j^{th}$ member (i.e., $H_1$).

Next the severity of damage in the $j^{th}$ member is estimated. Let the fractional change in the stiffness of the $j^{th}$ member be given by the severity estimator, $\alpha_j$, then by definition

$$E^*_j=E_j\,(1+\alpha_j) \tag{9}$$

Combining Eq. 7 and Eq. 9 yields

$$\alpha_j=1/\beta_j-1, \; \alpha_j\geq -1 \tag{10}$$

2.2 System Identification Method

Consider a linear skeletal structure with NE members and N nodes. Suppose $\mathbf{k}^*_j$ is an unknown stiffness of $j^{th}$ member of the structure for which M eigenvalues are known. Also, suppose $\mathbf{k}_j$ is a known stiffness of $j^{th}$ member of a finite element (FE) model for which the corresponding set of M eigenvalues are known. Then, relative to the FE model, the fractional stiffness change of the $j^{th}$ member of the structure, $\alpha_j$, and the stiffnesses are related according to the following equation (i.e., as shown in Eq. 9)

$$\mathbf{k}_j^*=\mathbf{k}_j\ (1+\alpha_j) \tag{11}$$

The fractional stiffness change of NE members is obtained by the following equation[8]

$$\alpha=\mathbf{F}^{-1}\mathbf{Z} \tag{12}$$

where $\alpha$ is a NE×1 matrix containing containing the fractional changes in stiffnesses between the FE-model and the structure, $\mathbf{Z}$ is a M×1 matrix containing the fractional changes in eigenvalues between them, and $\mathbf{F}$ is a M× NE damage sensitivity matrix relating the fractional changes in stiffnesses to the fractional changes in eigenvalues. This M×NE $\mathbf{F}$ matrix is determined in five steps : firstly, M undamaged eigenvalues are numerically generated from the FE model ; secondly, M damaged eigenvalues are numerically generated by introducing a known severity of damage at member j of the FE model ; thirdly, the fractional changes between M undamaged eigenvalues and M damaged eigenvalues are computed ; fourthly, each component of the column j of the $\mathbf{F}$ matrix (i.e., M×1 F matrix) is computed by dividing the fractional changes in each eigenvalue by the simulated severity at member j ; and finally, the M×NE $\mathbf{F}$ matrix is generated from repeating the whole procedure up to NE damage locations.

Using the above theory as a basis, the following 6-step algorithm are proposed to identify a certain structure :

1. Select a target structure (i.e., a post-damage state of the structure) ;
2. Select a FE model of the structure as an initial guess ;
3. Compute the damage sensitivity matrix of the FE model ;
4. Compute the fractional changes in eigenvalues between the FE model ad the target structure ; and
5. Fine-tune the FE model by first solving Eq. 12 to estimate stiffness changes (i.e., NE×1 matrix $\alpha$) and next solving Eq. 11 to update the stiffness parameters of the FE model.
6. Repeat Steps 1 to 5 until $\mathbf{Z}\cong 0$ or $\alpha\cong 0$ (i.e., as they approach zero) when the parameters of the FE model are identified.

2.3. Method to Quantify Model Uncertainty

In order to quantify the simulated model uncertainties which are either systematic (systematic error measures the degree to which an event occurs) or random (random error measures the accuracy of observations within an explicit model), a sensitivity assurance criterion (SAC) based on a metrical measure of modal energy changes is selected[9]. Consider two sampled patterns which are the uncertainty-free sensitivity vector $\mathbf{U}\in R^{NE}$ (i.e., Eq. 3 for a given mode) and the uncertainty-inflicted sensitivity vector $\mathbf{V}\in R^{NE}$, in which $R^{NE}$ is the space of order NE. Then the uncertainty measure, SAC, is defined as

$$\text{SAC}\ (\mathbf{U},\mathbf{V})=1-\mathbf{Cos}^2\ (\mathbf{U},\mathbf{V}),\ 0\le\text{SAC}\ (\mathbf{U},\mathbf{V})\le 1 \tag{13}$$

in which $\mathbf{Cos}\ (\mathbf{U},\mathbf{V})$ is the cosine of the angle between the two vectors

$$\mathbf{Cos}\ (\mathbf{U},\mathbf{V})=\frac{UV^T}{\|U\|\ \|V\|} \tag{14}$$

and quantify the differences in orientation between $\mathbf{U}$ and $\mathbf{V}$, without regard to scaling difficulties arising from choice of numerical distance units. If SAC $(\mathbf{U},\mathbf{V})=0$, then the vectors $\mathbf{U}$ and $\mathbf{V}$ are perfectly correlated (no uncertainty exists). If SAC $(\mathbf{U},\mathbf{V})>0$, then the vectors $\mathbf{U}$ and $\mathbf{V}$ become linearly unassociated

each other (uncertainty occurs).

2.4 Methods to Quantify Damage Detection Accuracy

The accuracy of damage prediction results is quantified by measuring both metrical errors and errors in hypothetical testing[9]. As the first NDD accuracy measure, a mean position error (MPE) is defined as

$$MPE\ (t,f)=\frac{1}{N}\sum_{i=1}^{N}|x_i^t-x_i^f|\ /L,$$
$$0\le MPE\ (t,f)\le 1 \qquad (15)$$

where N is the number of damage cases, $x_i^t$ is a true location of $i^{th}$ damage case, $x_i^f$ is a false location of $i^{th}$ damage case, and L is a certain distance (e.g., a span of a bridge). If MPE (t,f) is close to 1, then damage position error is close to the certain length L.

As the second NDD accuracy measure, a missing error (ME) is defined as

$$ME\ (t,f)=\frac{1}{NT}\sum_{i=1}^{N}\varepsilon_i^I,\ 0\le ME\ (t,f)\le 1 \qquad (16)$$

in which NT is the number of true damage locations and $\varepsilon_i^I$ is a Type I localization error ($\varepsilon_i^I=0$ if $i^{th}$ damage location is predicted or $\varepsilon_i^I=1$ if otherwise). If ME (t,f)=0, then all true damage locations are correctly located.

As the third NDD accuracy measure, a false alarm error (FAE) is defined as

$$FAE\ (t,f)=\frac{1}{NF}\sum_{i=1}^{N}\varepsilon_i^{II},\ 0\le FAE\ (t,f)<\infty \qquad (17)$$

in which NF is the number of predicted locations, $\varepsilon_i^{II}=1$ if otherwise). If FAE (t,f)=0, then all predicted locations are truly damaged locations.

As the last NDD accuracy measure, a mean sizing error (MSE) is defined as

$$MSE\ (t,f)=\frac{1}{NF}\sum_{i=1}^{N}|\ (\alpha_i^t-\alpha_i^f)\ /\alpha_i^t|,$$
$$0\le MSE\ (t,f)\le\infty \qquad (18)$$

where $\alpha_i^f$ is an estimated severity and $\alpha_i^t$ is a true damage severity of $i^{th}$ predicted location. If MSE (t,f) is close to 0, then the severity estimation error is close to 0.

## 3. DESIGN OF ASSESSMENT METHODOLOGY

The proposed assessment methodology has two design requirements. The first design requirement is that the methodology be able to estimate the relative impact of model uncertainty on the NDD accuracy in real structures. The second one is that the methodology be so general as to be applied to any structure for which measured modal responses of pre-damage and post-damage states are available. The second design requirement is satisfied automatically if the assessment methodology is independent of structure.

In order to satisfy these design requirements, the following thirteen components of the methodology are designed as shown in Fig. 1. Each components include at least one function which, if performed, will satisfy the requirements. Note that, in this study, the only requirement on the structure is that it be real and that modal data are available. The thirteen components shown in Fig. 1 are identified as follows.

Component 1. A real structure for which pre-damage and post-damage modal responses are available is selected.

Component 2. Modal responses including damage history, mode shapes, and frequencies of the real structure are identified.

Component 3. Damage detection models (DDMs) are selected on the basis of information about the topology, geometry, material properties, and modal responses of the structure. Here, damage detection model is defined as a mathematical representation of a structure with degrees of freedom corresponding to sensor readings.

Component 4. Damage localization and severity estimation in the structure are performed by using the proposed damage detection algorithm.

Component 5. Model uncertainty types which may exist in DDMs of a real structure are selected. Model uncertainty for NDD encompasses such causes as : (1) modeling errors in the choice of structure (or structural member) types, (2) inaccurate measurements of geometric and material properties, and (3) measurement noises, errors, and incompleteness in dynamic modal responses.

Component 6. A thoretical model of a real structure is generated by using the system identification method described in the previous section.

Component 7. Modal parameters of the theoretical model are generated. First, programmed damage is simulated to the theoretical model. Next, mode shapes and frequencies are numerically generated.

Component 8. An uncertainty-free DDM (i.e., a DDM based on complete knowledge on the theoretical model) is identified.

Component 9. For each uncertainty type selected in Component 5, model uncertainties of different severities are simulated to the theoretical model.

Component 10. Model uncertainties in the theoretical model are quantified by Eq. 13.

Component 11. First, damage in the theoretical model is located using the same procedures as defined in Component 4. Next, damage localization errors are quantified by using three NDD accuracy measures (i.e., Eqs. 15−17).

Component 12. First, damage severity in theoretical model is estimated using the same procedures as described in Component 4. Next, severity estimation errors are quantified by using a NDD accuracy measure (i.e., Eq. 18).

Component 13. Model uncertainties which have been tested against theoretical model are classified. Next, the effect of the uncertainties on the damage detection accuracy are compared.

## 4. UNCERTAINTY ASSESSMENT OF DAMAGE PREDICTION ACCURACY

The feasibility of the assessment methodology presented in the previous section is demonstrated by using a plate-girder bridge for which only information on a single mode is available. The accuracy of NDD results of the plate-girder bridge is quantified as a function of model uncertainties which are most likely or existing in the damage prediction procedure of the bridge. Hereafter, tasks to fulfill each component shown in Fig. 1 will be performed.

### 4.1 Damage Detection in a Plate-Girder Bridge

The test structure, a two-span aluminum plate-girder bridge, is shown in Fig. 2. Mazurek and DeWolf[10] conducted controlled laboratory experiments on the bridge to measure changes in modal responses caused by structural degradation. As shown in Fig. 2, the bridge consisted of plates and angle shapes, bolted together to form two I-section girders. The bridge had three supports : a pin support six inches (0.15m) from the left edge, a roller sup-

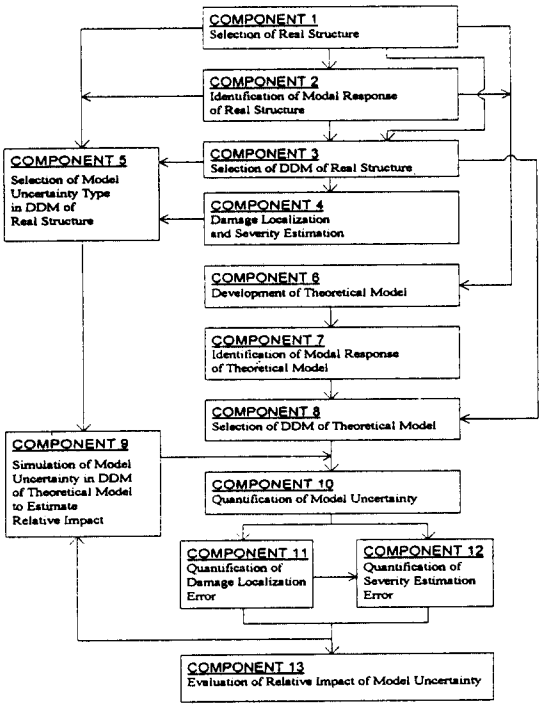


Fig. 1 Schematic of Method to Assess Model Uncertainty Vs NDD Accuracy
(Note : origins of each arrow are input data to components to which the arrow heads.)

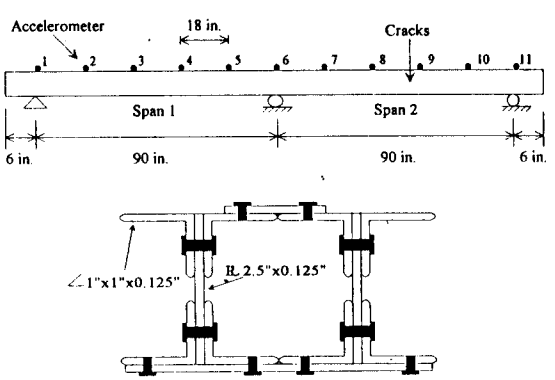


Fig. 2 Schematic of the Plate-Girder Bridge

port at the middle, and another roller support six inches (0.15 m) from the right edge. Eleven accelerometers were placed along the surface of the bridge and the ambient vibration method was used to obtain modal responses of the bridge.

A known damage was inflicted by cracking the girder at a location 40 inch to the left of the right support. The crack (i.e., the inflicted damage) was placed on the right web shown in Fig. 2. The crack was devloped further in three damage stages, reducing the bending stiffness at the crack location to about 19 percent (Stage 1), 32 percent (Stage 2), and 33 percent (Stage 3) of that of the original cross-section. The extracted modal parameters of the bridge include mode shapes of the first bending mode (shown in Fig. 3) and resonant frequencies of the first three bending modes (listed in Table 1). Note that the mode shapes used in this study were obtained by digitizing the mode shapes presented in Reference[10].

As a damage detection model (DDM) of the bridge, an Euler-Bernoulli beam model was selected since (1) the bridge consists of a box girder that can be modeled as a beam and (2)

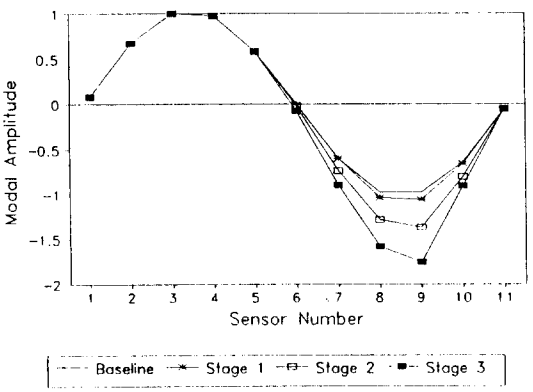


Fig. 3 Mode Shapes of the Plate-Girder Bridge

Table 1. Resonant Frequencies (Hz) of the Plate-Girder Bridge

| Damage Stage | Model 1 | Model 2 | Model 3 |
|---|---|---|---|
| Undamaged | 32.32 | 46.58 | 118.1 |
| 1 | 32.02 | 45.98 | 116.1 |
| 2 | 30.96 | 45.38 | 115.7 |
| 3 | 29.01 | 45.07 | 115.5 |

the collected modal data provide information that can be used to model a one-dimensional structure (i.e., the bridge has accelerometers which measure only vertical motions). The DDM consisted of 50 beam elements of equal size (i.e., each element space equally between two adjacent nodes) and the modal strain energy of an element connecting two nodes (a,b) is given by $\int_a^b EI\{\phi''(x)\}^2 dx/2$. For each element, we estimated geometric and material properties as follows : (1) the elastic modulus $E=10\times10^6$ psi (70 Gpa), (2) Poisson's ratio $\upsilon=0.33$, (3) the second moment of area $I=1.737$ in$^4$ ($7.23\times10^{-7}$m$^4$), and (4) the linear mass density $\rho=2.537\times10^{-4}$lb · s$^2$/in$^4$ (271( /m$^3$). Next, the curvatures of the mode shapes were generated at the 51 nodes of the damage detection model. For the undamaged structure and three damaged structures (note that each mode shape shown in Fig. 3 contained only 11 sensor readings), the curvatures were obtained in three steps. Firstly, values of the modal amplitudes corresponding to Nodes 1-51 were estimated by interpolating, using cubic-spline functions, the mode shapes shown in Fig. 3. Secondly, a modal displacement function, w (x), was generated for the entire structure using third-order interpolation functions. Thirdly, the curvature, $\phi''(x)=d^2w(x)/dx^2$, was determined at 51 nodes of the damage detection model.

Next, for the three damage stages, damage in the bridge was located and sized in five steps. Firstly, as the input data to the damage detection model, the mode shapes and resonant frequencies of the first bending mode were used. Secondly, the damage index (given by Eq. 7) of the damage detection model (i.e., the Euler-Bernoulli beam model) was computed for each damage stage. Thirdly, the damage localization criterion (given by Eq. 8) was established as follows : (1) select $H_0$ if $Z_i<2$ (i.e., no damage exists at member i) and (2) select the alternate $H_1$ if $Z_i\geq2$. This criterion corresponds to a one-tailed test at a significance level of 0.023 (97.7 percent confidence level). Fourthly, the criterion was used to select potential damage locations. The inflicted (i.e., actual) and predicted damage locations for the three damage stages are shown in Fig. 4. Finally, for each predicted damage location, severity of damage was estimated using the procedure outlined in Eqs. 9-10. The inflicted and estimated severities of damage are listed

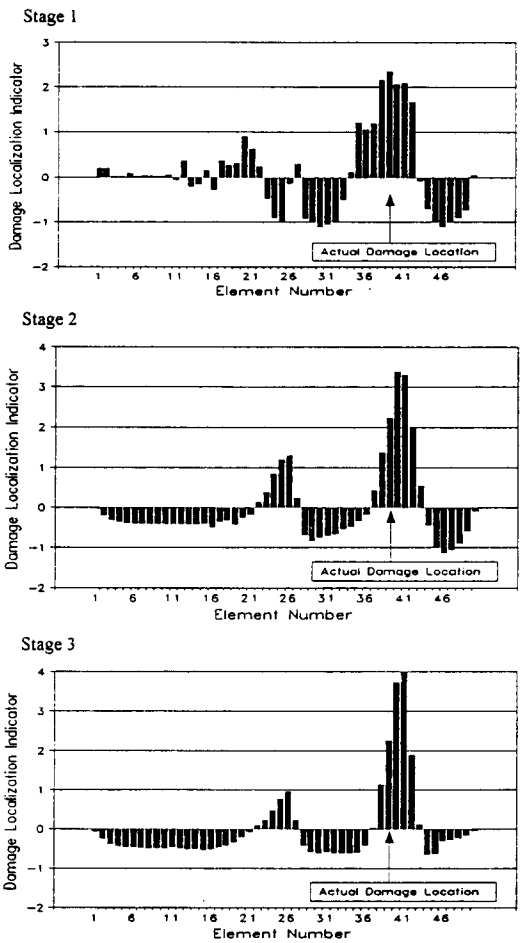


Fig. 4 Damage Localization Results of the Plate-Girder Bridge

Table 2. Severity Estimation Results of the Plate-Girder Bridge

| Damage Stage | Damage Element | Severity of Damage | |
|---|---|---|---|
| | | Inflicted | Predicted |
| 1 | 39 | −19% | −49% |
| 2 | 39 | −32% | −58% |
| 3 | 39 | −33% | −70% |

in Table 2. A negative value in Table 2 represents the reduction in stiffness.

From the damage localization and severity estimation results, the following three-results are observed. Firstly, for all levels of damage (i.e., Stage 1 to Stage 3), damage is indicated either at or in the vicinity of element 39 (i.e., the actual damage location). Secondly, the precision of the damage localization increases as the level of the inflicted damage increases. Thirdly, the predicted severity estimation results consistently oversestimate the inflicted damage..

4.2 Identification of the Theoretical Model

The theoretical model of the plate-girder bridge was identified by implementing the 6-step system identification algorithm described previously. Firstly, the first damage case (i.e., the Stage 1) of the plate-girder bridge was selected as the target structure. Secondly, a beam FE model was selected as an initial guess. As shown in Fig.5, the FE model consisted of three members as follows : Member 1 for 50 equally sized beam elements, Member 2 for the two outside axial springs (Spring 1), and Member 3 for the middle axial spring (Spring 2). Geometric properties of the FE model were initially assigned as : (1) for Member 1, $A=1.625in^2$ ($1.05\times10^{-3}m^2$) and $I=1.737in^4$ ($7.23\times10^{-7}m^4$) and (2) for Members 2 and 3, $A=0.1in^2$ ($6.45\times10^{-5}m^2$) and $I\approx0$. Next, material properties of all members were assigned as : (1) the elastic modulus $E=10\times10^6$ psi (70 Gpa), (2) Poisson's ratio $\upsilon=0.33$, and (3) the linear mass density $\rho=2.537\times10^{-4}lb\cdot s^2/in^4$ ($2710kg/m^3$). Thirdly, a numerically generated **F** matrix of the FE model is listed in Table 3. For a given mode, each sensitivity represents the fraction of modal energy of that mode stored in the particular member. Finally, we obtained a fine-tuned FE model. The results of implementing the system identification method, using three frequencies and ten iterations, are listed in Table 4. After tenth iterations the identified frequencies are within one percent of the target values. The FE model of the tenth iteration is selected as the theoretical model. As the stiffness parameters, bending rigidity was used for Member 1 and axial rigidity was used for Members 2 and 3.

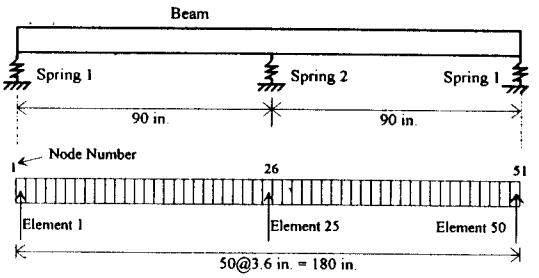


Fig. 5 Schematic of the FE Model of the Plate-Girder Bridge

Table 3. Sensitivity Matrix to Fine-Tune the Finite Element Model

| Mode | Sensitivity of Members | | |
|---|---|---|---|
| | Member 1 | Member 2 | Member 3 |
| 1 | 0.9995 | 0.5E-3 | 0.1E-4 |
| 2 | 0.9950 | 0.1E-2 | 0.4E-2 |
| 3 | 0.9979 | 0.2E-2 | 0.1E-3 |

Table 4. Values of Frequencies (Hz) for Ten Iterations

| Mode Number | Initial Guess | 2nd Iteration | 4th Iteration | 6th Iteration | 8th Iteration | 10th Iteration | Target Values |
|---|---|---|---|---|---|---|---|
| 1 | 39.76 | 32.63 | 32.54 | 32.45 | 31.37 | 32.29 | 32.06 |
| 2 | 61.99 | 44.60 | 45.15 | 45.47 | 45.63 | 45.76 | 45.98 |
| 3 | 158.75 | 121.32 | 120.07 | 119.18 | 118.15 | 117.13 | 116.10 |

4.3 Modal Responses of the Theoretical Model

Frequencies and mode shapes of the identified theoretical model were generated via numerical simulation using the software package ABAQUS[11]. Here, nine damage scenarios are programmed with inflicted damage at different elements of the FE model shown in Fig. 5. The simulated locations and their corresponding inflicted damage are summarized in Table 5. The first six damage cases were limited to the theoretical model damaged only at a single location and the remaining three cases considered damage inflicted at two locations. The first three frequencies of the initial structure and the nine damage structures are listed in Table 6. Typical numerically generated mode shapes of the first three modes are shown in Fig. 6.

4.4 Simulation of Model Uncertainty to the Theoretical Model

Four model uncertainty types were first selected from the damage detection procedure of the plate-girder bridge and later simulated to

Table 5. Damage Scenarios for the Theoretical Model

| Case | Element | Damage | Case | Element | Damage | Case | Element | Damage |
|---|---|---|---|---|---|---|---|---|
| 1 | 4 | -10% | 4 | 19 | -10% | 7 | 4,29 | -10%, -10% |
| 2 | 9 | -10% | 5 | 24 | -10% | 8 | 9,34 | -10%, -10% |
| 3 | 14 | -10% | 6 | 39 | -10% | 9 | 14,39 | -10%, -10% |

Table 6. Natural Frequencies (Hz) of the Theoretical Model

| Case | Mode 1 | Mode 2 | Mode 3 |
|---|---|---|---|
| Undamaged | 32.381 | 46.377 | 118.77 |
| 1 | 32.368 | 46.356 | 118.66 |
| 2 | 32.328 | 46.309 | 118.69 |
| 3 | 32.314 | 46.331 | 118.74 |
| 4 | 32.346 | 46.376 | 118.58 |
| 5 | 32.379 | 46.282 | 118.75 |
| 6 | 32.179 | 46.188 | 118.77 |
| 7 | 32.356 | 46.325 | 118.54 |
| 8 | 32.276 | 46.297 | 118.52 |
| 9 | 32.247 | 46.266 | 118.74 |

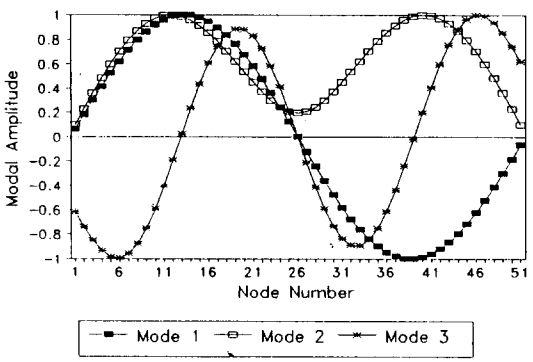


Fig. 6 Mode Shapes of the Theoretical Model

the theoretical model. As the first type, the uncertainty in the DDM selection was selected because the Euler-Bernoulli beam model (which was used for the damage prediction for the bridge) represented only estimates of the modal energy of incomplete parameters of the bridge. This uncertainty was simulated to the theoretical model by varying the choice of DDM to the following forms such as : (1) the FE model (i.e., the theoretical model itself) as an uncertainty-free DDM and (2) the Euler-Bernoulli beam model as an uncertainty-inflicted DDM.

As the second type, the uncertainty in the stiffness parameter was selected since the true stiffness parameters of the bridge were unknown. This uncertainty was simulated by introducing log-normal distributions (in terms of the coefficient of variation (COV)) of elastic moduli to element stiffnesses of the FE model. Four different uncertainties were programmed as follows : (1) the uncertainty-free FE model, (2) the FE model with 10% COV, (3) the FE model with 30% COV, and (4) the FE model with 50% COV.

As the third type, the uncertainty in the mode shape was selected since the mode shapes used for the damage prediction of the bridge contained errors due to digitizing the orig-

inal mode shapes and interpolating the digitized mode shapes. This uncertainty (which is random) was simulated by introducing normal distributions (in terms of the COV) of modal amplitudes to the mode shapes of the FE model. Seven different uncertainties were programmed as follows : (1) the uncertainty-free FE model, (2) the FE model with 0.01% COV, (3) the FE model with 0.05% COV, (4) the FE model with 0.1% COV, (5) the FE model with 0.15% COV, (6) the FE model with 0.2% COV, and (7) the FE model with 3% COV. The minimum and maximum COV values were estimated from the differences between the undamaged mode shape and the nine damaged mode shapes of the theoretical model. To illustrate the effect of variations of the normal or log-normal distributions, Monte Carlo simulations were employed to obtain statistically meaningful results.

As the final type, the uncertainty in the frequency was selected since the measured resonant frequencies contained approximately 11 percent maximum error. This uncertainty in the frequency (random uncertainty) was simulated by reducing the frequencies of the FE model. Four uncertainties were programmed as follows : (1) the uncertainty-free FE model, (2) the FE model with 10% reduction, (3) the FE model with 30% reduction, and (4) the FE model with 50% reduction.

### 4.5 Quantification of Model Uncertainty and Damage Prediction Accuracy

The uncertainty measure of Eq. 13 (i.e., SAC) was used to quantify each uncertainty in the theoretical model. The sensitivity vectors were computed by using Eq. 3 for the first bending mode. First, uncertainty-free sensitivity vectors were computed from the FE model. Next, for each uncertainty, uncertainty-inflicted sensitivity vectors were computed from the uncertainty-inflicted DDM. Results for the four uncertainty types are listed in Table 7. From Table 7, four major results on the uncertainty quantification are observed. Firstly, SAC is very small for the uncertainty in the DDM selection. Secondly, SAC increases when the uncertainty in the stiffness parameter increases. Thirdly, SAC increases highly even when the uncertainty in the mode shape increases very little. Fourthly, SAC does not change for the uncertainty in the frequency.

Table 7. Quantification of Model Uncertainties in the Theoretical Model

| Uncertainty Type | Simulated Uncertainty | SAC |
|---|---|---|
| DDM Selection | FE Model(Uncertainty-Free) | 0.000 |
| DDM Selection | Euler-Bernoulli Beam Model | 0.010 |
| Stiffness Parameter | FE Model+10% COV | 0.114 |
| Stiffness Parameter | FE Model+30% COV | 0.332 |
| Stiffness Parameter | FE Model+50% COV | 0.510 |
| Mode Shape | FE Model+0.01% COV | 0.003 |
| Mode Shape | FE Model+0.05% COV | 0.032 |
| Mode Shape | FE Model+0.10% COV | 0.118 |
| Mode Shape | FE Model+0.15% COV | 0.228 |
| Mode Shape | FE Model+0.20% COV | 0.336 |
| Mode Shape | FE Model+0.30% COV | 0.503 |
| Frequency | FE Model+10% Reduction | 0.000 |
| Frequency | FE Model+30% Reduction | 0.000 |
| Frequency | FE Model+50% Reduction | 0.000 |

Next, for each uncertainty listed in Table 6, damage prediction accuracy was quantified. First, damage localization and severity estimation in the theoretical model were performed using the same procedure as described previously. By implementing the four NDD accuracy measures of Eqs. 15-18 to the damage localization and severity estimation results, the NDD accuracy was quantified, as listed in Table 8. From Table 8, four major results to the NDD accuracy are observed. Firstly, for the uncertainty in the selection of the Euler-Bernoulli beam model as a DDM, the

Table 8. Quantification of the NDD Accuracy of the Theoretical Model

| Uncertainty Type | Simulated Uncertainty | MPE | ME | FAE | MSE |
|---|---|---|---|---|---|
| DDM Selection | FE Model(Uncertainty-Free) | 0.000 | 0.000 | 0.000 | 0.808 |
| DDM Selection | Euler-Bernoulli Beam Model | 0.030 | 0.083 | 0.250 | 0.229 |
| Stiffness Parameter | FE Model+10% COV | 0.000 | 0.000 | 0.000 | 0.808 |
| Stiffness Parameter | FE Model+30% COV | 0.000 | 0.000 | 0.000 | 0.808 |
| Stiffness Parameter | FE Model+50% COV | 0.000 | 0.000 | 0.000 | 0.808 |
| Mode Shape | FE Model+0.01% COV | 0.000 | 0.000 | 0.050 | 0.807 |
| Mode Shape | FE Model+0.05% COV | 0.121 | 0.220 | 0.140 | 0.864 |
| Mode Shape | FE Model+0.10% COV | 0.368 | 0.520 | 0.040 | 1.004 |
| Mode Shape | FE Model+0.15% COV | 0.546 | 0.635 | 0.015 | 1.073 |
| Mode Shape | FE Model+0.20% COV | 0.646 | 0.710 | 0.050 | 1.116 |
| Mode Shape | FE Model+0.30% COV | 0.648 | 0.735 | 0.000 | 1.524 |
| Frequency | FE Model+10% Reduction | 0.000 | 0.000 | 0.000 | 0.808 |
| Frequency | FE Model+30% Reduction | 0.000 | 0.000 | 0.000 | 0.808 |
| Frequency | FE Model+50% Reduction | 0.000 | 0.000 | 0.000 | 0.808 |

NDD accuracy measures show : (1) MPE of 0.03 (i.e., damage under the given conditions can be predicted with a position error of 3 percent of the bridge length) ; (2) ME of 0.083 (i.e., eleven among twelve damage locations under the given conditions can be predicted correctly) ; (3) FAE of 0.25 (i.e., one of the four predicted locations can be false-positive) ; and (4) MSE of 0.23 (i.e., an average severity estimation error of 23 percent). Secondly, for the uncertainty in the stiffness parameter, the NDD accuracy measures do not change. Note that the NDD theory used in this study is independent of material properties. Thirdly, when the uncertainty in the mode shape increases, the NDD accuracy measures show : (1) MPE, ME, and MSE values consistently increase and (2) FAE increase or decrease. Finally, the NDD accuracy measures do not change for the uncertainty in the frequency. Note that only a single mode was used in the damage prediction of 50 elements of the structure.

4.6 Estimation of Relative Impact of Model Uncertainty on the NDD Accuracy

| Uncertainty Type | Simulated Uncertainty | Uncertainty Measure (SAC) | NDD Accuracy Measures | | | |
|---|---|---|---|---|---|---|
| | | | MPE | ME | FAE | MSE |
| DDM Selections | FE Model | NO | NO | NO | NO | ST |
| | Euler Beam Model | WK | WK | WK | ST | ST |
| Stiffness Parameters | COV=10% | ST | NO | NO | NO | ST |
| | COV=30% | ST | NO | NO | NO | ST |
| | COV=50% | ST | NO | NO | NO | ST |
| Mode Shapes Due to Errors in Modal Amplitudes | COV=0.01% | WK | NO | NO | WK | ST |
| | COV=0.05% | WK | ST | ST | ST | ST |
| | COV=0.10% | ST | ST | ST | WK | ST |
| | COV=0.15% | ST | ST | ST | WK | ST |
| | COV=0.20% | ST | ST | ST | WK | ST |
| | COV=0.30% | ST | ST | ST | NO | ST |
| Frequencies | 10% Reduction | NO | NO | NO | NO | ST |
| | 30% Reduction | NO | NO | NO | NO | ST |
| | 50% Reduction | NO | NO | NO | NO | ST |

Fig. 7 NDD Accuracy as a Function of Model Uncertainty in the Theoretical Model

(Note : ST-Strong Influence (Value>0.1), WK-Weak Influence (0<Value<0.1), and NO-No Influence (Value=0))

The relative impact of model uncertainty on the NDD accuracy is evaluated from the uncertainty assessment results shown in Tables 7 and 8. Fig. 7 shows the relationships between the model uncertainty types, the uncertainty measure, and the four NDD accuracy measures. Firstly, the selection of the Euler-Bernoulli beam model as a DDM causes a weak uncertainty. This uncertainty has a weak influence on MPE and ME and a strong influence on FAE and MSE. Secondly, the variations in element stiffnesses of the FE model cause relatively strong uncertainties. However, this uncertainty type has no influence on MPE, ME, FAE, and MSE. Thirdly, the variations in mode shapes of the FE model cause strong uncertainties. This uncertainty type has a strong influence on MPE, ME, and MSE but a relatively weak influence on FAE. Finally, the frequency changes of the FE model cause no uncertainty and no influences on the NDD accuracy measures.

## 5. SUMMARY AND CONCLUSIONS

The objective of this study was to present a methodology to assess the relative effect of model uncertainty on the accuracy of damage detection in structures. The investigation was performed in three parts. Firstly, a theory of damage localization and severity estimation were outlined and a system identification method to generate a theoretical model of a structure was formulated. Secondly, a methodology to assess the effect of model uncertainty on the damage detection accuracy of real structures was designed. Finally, the feasibility of the proposed methodology was demonstrated by using a plate-girder bridge for which only information on a single mode is available.

By applying the approach to the model bridge, the following relationships between model uncertainty and the damage prediction accuracy were obtained : (1) an uncertainty caused by selecting the Euler-Bernoulli beam model as the damage detection model had a relatively weak influence on the damage prediction accuracy ; (2) uncertainties in the mode shapes had relatively strong influences on the damage prediction accuracy ; and (3) uncertainties in the stiffness parameter and uncertainties in the frequencies had no influence on the damage prediction accuracy.

From the results of this study, it is concluded that a methodolgy to evaluate damage prediction accuracy as a function of model uncertainty in structure has been developed. As a significant contribution, this proposed method may improve the effectivenes of future damage detection tests on real structures. For example, the proposed method can determine beforehand what data must be gathered to produce pre-determined level of damage prediction accuracy. Future research efforts are needed in several directions. Firstly, it is necessary to apply the assessment methodology of this study to different classes of structures. Secondly, it is also necessary to apply this methodology to other damage detection methods. Thirdly, it is necessary to verify the uncertainty assessment predictions by performing more laboratory and field experiments.

## REFERENCES


1. Cawley, P. and Adams, R.D., "The Location of Defects in Structures from Measurements of Natural Frequencies", J. Strain Analysis, Vol.14, No.2, pp.49-57, 1979.
2. O'Brien, T.K., "Stiffness Change As A Non-destructive Damage Measurement", Mechanics of Non-destructive Testing, ed. W.W. Stinchcomb, Plenum Press, pp.101-121, 1980.
3. Gudmunson, P., "Eigenfrequency Changes of Structures Due to Cracks, Notches or Other Geometrical Changes", J. Mech. Phys. Solids, Vol.30, No.5, pp.339-353, 1982.
4. Biswas, M., Pandey, A.K. and Samman, M., "Modal Technology for Damage Detection of Bridges", NATO Workshop on Bridge Evaluation, Repair and Rehabilitation, ed. A. Nowak, Kluwer Academic Publishers, Maryland, pp.161-174, 1990.
5. Stubbs, N. and Osegueda, R., "Global Non-Destructive Damage Evaluation in Solids', Int. J. Anal. Exp. Modal Analysis, Vol.5, No.2, pp.67-79, 1990.
6. Beck, J.L. and Katafygiotis, L.S., "Updating of a Model and Its Uncertainties Utilizing Dynamic Test Data", Computational Stochastic Mechanics, eds. P.D. Spanos and C.A. Brebbia, Elsevier Applied Science, London, pp. 125-135, 1991.
7. Stubbs, N., Kim, J.T. and Topole, K., "An Efficient and Robust Algorithm for Damage Localization in Offshore Platforms", ASCE Tenth Structures Congress '92, San Antonio, Texas, pp.543-546, 1992.
8. Stubbs, N., Kim, J.T. and Topole, K., "The

Effect of Model Uncertainty on the Accuracy of Global Nondestructive Damage Detection in Structures", Computational Stochastic Mechanics, eds. P.D. Spanos and C.A. Brebbia, Elsevier Applied Science, London, pp. 157-168, 1991.

9. Kosko, B., Neural Networks and Fuzzy Systems, Prentice Hall, New Jersey, 1992.
10. Mazurek, D.F. and DeWolf, J.T., "Experimental Study of Bridge Monitoring Technique", J. of Structural Engineering, ASCE, Vol.116, No.9, pp.2532-2549, 1990.
11. Kosko, B., Neural Networks for Signal Processing, Prentice Hall, New Jersey, 1992.
12. ABAQUS User Manual (1987), Hibbitt, Karlsson & Sorensen, Inc.

(接受 : 1994. 5. 6)